KKU SCIENCE JOURNAL

Journal Home Page : https://ph01.tci-thaijo.org/index.php/KKUSciJ

Published by the Faculty of Science, Khon Kaen University, Thailand

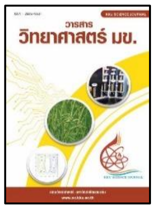

ผลกระทบของการลด Cu และเพิ่ม Ti ต่อโครงสร้างทางจุลภาคและสมบัติทางไจแอนท์ไดอิเล็กทริกของวัสดุเซรามิก $CaCu_3Ti_4O_{12}$

Effects of Cu-deficiency and Ti-excess on Microstructure and Giant Dielectric Properties of $CaCu_3Ti_4O_{12}$ Ceramics

ปิยะนุช วงศ์ทองดี[1] และ ประสิทธิ์ ทองใบ[1,2*]

Piyanud Wongtongdee[1] and Prasit Thongbai[1,2*]

[1]กลุ่มวิจัยวัสดุไจแอนท์ไดอิเล็กทริกและการออกแบบคำนวณ สาขาวิชาฟิสิกส์ คณะวิทยาศาสตร์ มหาวิทยาลัยขอนแก่น จังหวัดขอนแก่น 40002

[2]สถาบันวิจัยและนวัตกรรมวัสดุนาโนเพื่อพลังงาน มหาวิทยาลัยขอนแก่น จังหวัดขอนแก่น 40002

[1]Giant Dielectric and Computational Design Research Group (GD–CDR), Department of Physics, Faculty of Science, Khon Kaen University, Khon Kaen 40002, Thailand

[2]Institute of Nanomaterials Research and Innovation for Energy (IN-RIE), Khon Kaen University, Khon Kaen 40002, Thailand

บทคัดย่อ

การสังเคราะห์วัสดุเซรามิก $CaCu_{3-x}Ti_{4+x}O_{12}$ ที่มี x = 0 (CCTO) และ 0.09 (CCTO-C/T) โดยใช้วิธีปฏิกิริยาสถานะของแข็ง โดยมีวัตถุประสงค์เพื่อสำรวจอิทธิพลของการลด Cu และเพิ่ม Ti ที่ส่งผลต่อโครงสร้างจุลภาคและคุณสมบัติไดอิเล็กทริกของวัสดุเซรามิก CCTO ซึ่งตรวจพบเฟสหลักของ CCTO ที่ได้รับการยืนยันการเกิดเฟสโดยไม่คำนึงถึงความเบี่ยงเบนของอัตราส่วนโมลาร์ของ Cu และ Ti ในวัสดุเซรามิก CCTO-C/T แสดงเฟสทุติยภูมิของ TiO_2 และการแยกตัวของ CuO ตามขอบเกรน การปรับอัตราส่วนระหว่าง Cu และ Ti นั้นขัดขวางการเจริญเติบโตของเกรนในวัสดุเซรามิก CCTO-C/T ผลการศึกษาสมบัติทางไดอิเล็กทริกพบว่า วัสดุเซรามิก CCTO และ CCTO-C/T มีการตอบสนองทางไดอิเล็กทริกที่สูงมาก โดยมีค่าคงที่ไดอิเล็กทริกในระดับ 10^4 และวัสดุเซรามิก CCTO-C/T มีค่าแทนเจต์ของการสูญเสียที่ต่ำกว่าเมื่อเทียบกับวัสดุเซรามิก CCTO จากผลการศึกษาด้วยเทคนิคอิมพีแดนซ์สเปกโทรสโกปี ได้ยืนยันตอบสนองทางไฟฟ้าที่แตกต่างกันระหว่างเกรนที่เป็นสารกึ่งตัวนำและฉนวนบริเวณของขอบเกรน ความต้านทานขอบเกรนของวัสดุเซรามิก CCTO-C/T สูงกว่าวัสดุเซรามิก CCTO ซึ่งเป็นผลมาจากการเกิดเฟส CuO ตามแนวนขอบเกรน และเฟส TiO_2 ที่มาก ส่งผลให้ความเข้มข้นของอิเล็กตรอนอิสระภายในเกรนสารกึ่งตัวนำของเซรามิก CCTO-C/T จึงลดลง และการตอบสนองของไดอิเล็กทริกลดลง การศึกษานี้ให้ข้อมูลเชิงลึกเกี่ยวกับปัจจัยที่มีอิทธิพลต่อโครงสร้างจุลภาคและคุณสมบัติไดอิเล็กทริกของเซรามิก CCTO และ CCTO-C/T ซึ่งช่วยเพิ่มความเข้าใจของเราเกี่ยวกับวัสดุเหล่านี้และการใช้งานที่เป็นไปได้ในด้านเทคโนโลยีต่างๆ

*Corresponding Author, E-mail: pthongbai@kku.ac.th

Received: date: 8 July 2023 | Revised date: 29 August 2023 | Accepted date: 13 September 2023

ABSTRACT

$CaCu_{3-x}Ti_{4+x}O_{12}$ ceramics with x = 0 (CCTO) and 0.09 (CCTO-C/T) were synthesized using the solid-state reaction method. The objective was to explore the influence of Cu-deficiency and Ti-excess on the microstructure and dielectric properties of CCTO ceramics. The presence of the primary CCTO phase was confirmed, regardless of deviations in the Cu and Ti molar ratios. The CCTO-C/T ceramic exhibited a secondary phase of TiO_2 and segregation of CuO along the grain boundaries. Adjustment of the Cu and Ti ratios hindered grain growth in the CCTO-C/T ceramic. Some CuO segregation along grain boundaries and deficiencies in Ti and Ca were observed in the CCTO-C/T ceramic. Notably, both CCTO and CCTO-C/T ceramics demonstrated a remarkable giant dielectric response of 10^4. The CCTO-C/T ceramic exhibited a lower loss tangent compared to the CCTO ceramic. Impedance spectroscopy confirmed electrical heterogeneity, with distinct electrical responses attributed to semiconducting grains and insulating grain boundaries. The grain boundary resistance of the CCTO-C/T ceramic was higher than that of the CCTO ceramic, attributed to the presence of segregated CuO and excessive TiO_2 phases. Consequently, the concentration of free electrons within the semiconducting grains of the CCTO-C/T ceramic decreased, resulting in a decrease in the giant dielectric response. This study provides valuable insights into the factors influencing the microstructure and dielectric properties of CCTO and CCTO-C/T ceramics, enhancing our understanding of these materials and their potential applications in various technological fields.

คำสำคัญ: การตอบสนองทางไดอิเล็กทริกขนาดใหญ่ ขอบเกรน ตัวเก็บประจุแบบขวางกั้น เทคนิคอิมพีแดนซ์สเปกโทรสโกปี

Keywords: Giant/Colossal Permittivity, Grain Boundary, Internal Barrier Layer Capacitor, Impedance Spectroscopy

INTRODUCTION

$CaCu_3Ti_4O_{12}$ (CCTO) is a captivating material that has garnered significant attention in the fields of condensed matter physics and materials science (Subramanian *et al.*, 2000; Adams *et al.*, 2006; Miao *et al.*,2021; Bhardwaj *et al.*, 2022; Jumpatam *et al.*, 2022). It belongs to the family of complex perovskite oxides of $\mathbf{A}Cu_3Ti_4O_{12}$ ceramics, where **A** represents divalent cation or averaged divalent cations, such as Ca^{2+}, $Bi^{3+}_{2/3}$, $Na^{+}_{1/2}Y^{3+}_{1/2}$, or $Na^{+}_{1/2}Bi^{3+}_{1/2}$) (Subramanian and Sleight, 2002; Rai *et al.*, 2022; Saengvong *et al.*, 2022), showing extraordinary dielectric properties. CCTO is known for its remarkably high dielectric constant ($\varepsilon' > 10^4$), making it a potential candidate for various technological applications (Moulson and Herbert, 2003).

The crystal structure of CCTO consists of alternating layers of copper (Cu^{2+}), calcium (Ca^{2+}), and titanium (Ti^{4+}) ions, arranged in a cubic perovskite lattice. Such a high dielectric constant is extremely rare among known materials and has sparked interest in exploiting CCTO for high-capacitance applications, such as energy storage devices, capacitors, and microwave components (Moulson and Herbert, 2003). Unfortunately, the dielectric loss tangent was very large ($\tan\delta > 0.1$), which is unsuitable for electronic applications (Zhang *et al.*, 2019; Jumpatam *et al*., 2022). A large tanδ in CCTO, despite its remarkable electrical properties, can pose certain challenges and limitations in practical applications. The loss tangent represents the ratio of the energy dissipated as heat to the stored energy in a material when an electric field is applied. In the case of CCTO, although it possesses a high dielectric constant and low energy loss, it is also known to have a relatively large loss tangent.

For CCTO ceramics, the observed abnormal grain growth was likely due to the liquid phase sintering mechanism (Mei *et al*., 2008; Vangchangyia *et al*., 2012). The source of liquid that existed during the sintering at a high temperature was related to CuO (Lee *et al*., 2014). Abnormal grain growth in CCTO ceramics often results in a distribution of grain sizes, which can exhibit a bimodal nature with both large and small grains. The dc current (movement of free charge carriers) deviates within the ceramic as it avoids the fine–grained regions. This diversion occurs due to the high impedance associated with the increased density of grain boundaries in those regions (Adams *et al.*, 2006). Thus, a large number of free charges passing through the large grain region gives rise to an increase in DC conductivity and tanδ value. To mitigate the substantial enlargement of grain size, the molar ratio of CuO in CCTO must be reduced. Another method to decrease the enlarged grain growth is to increase the molar ratio of TiO_2 (Lin *et al*., 2008; Saengvong *et al*., 2021). In this case, it was observed that the average grain size decreased with an increase in the molar ratio of TiO_2. Furthermore, the segregation of the TiO_2 phase can contribute to an increase in the resistance of the grain boundaries in CCTO ceramics (Saengvong *et al*., 2021). The aim of this research work is to reduce the tanδ value by employing a combination method that involves simultaneously decreasing the CuO ratio and increasing the TiO_2 ratio.

In this work, $CaCu_{3-x}Ti_{4+x}O_{12}$ ceramics were synthesized using a solid-state reaction method. The effects of Cu and Ti molar ratios on phase formation, microstructure, and dielectric properties were studied. The origins of the variations in the giant dielectric properties were discussed in detail.

MATERIALS AND METHODS

In this study, the synthesis of $CaCu_{3-x}Ti_{4+x}O_{12}$ ceramics with x = 0 (CCTO) and 0.09 (CCTO–C/T) was conducted using a solid-state reaction method. It has been reported that Ti ions can be substituted into the Cu site within the CCTO structure (Adams *et al.*, 2006). If this holds true, for the sample with x = 0.09, approximately 3 at % of the Cu sites could potentially be replaced by Ti ions. The starting raw materials, i.e., $CaCO_3$ (99.9%), CuO (99%) and TiO_2 (99.9%), were first combined. Subsequently, a ball-milling technique was employed, with ZrO_2 balls used as grinding media, to mix the starting materials in ethanol for 24 h. Following the milling process, the mixture was separated from the ZrO_2 balls and ethanol evaporated at 90 °C for 24 h. The resulting dried powders were carefully ground and underwent calcination at 800 °C for 5 h. using heating and cooling rates of 5 °C/min. Careful grinding was then performed to obtain a fine and homogeneous calcined powder. Afterward, pellets were shaped by compressing ceramic powders for all compositions at 250 MPa using uniaxial compressive strength. Finally, the pellets were sintered at 1,090 °C for 5 h. at a heating rate of 5 °C/min, followed by natural cooling to room temperature.

The sintered ceramics were characterized using X-ray diffraction (XRD, PANalytical, EMPYREAN), field-emission scanning electron microscopy (FE-SEM) with energy-dispersive X-ray analysis (EDS) (HITACHI SU8030, Japan) and SEM-mapping technique were employed to systematically characterize the sintered specimens. To acquire SEM images of the surface morphologies, both samples underwent polishing and thermal etching. Comprehensive details of each technique are provided in our previous published work (Prachamon *et al.*, 2022). The dielectric properties were tested. Silver paint was coated on both sides of the polished samples and heated at 600 °C for 30 min. The dielectric parameters were measured using a KEYSIGHT E4990A Impedance. The measurement was performed in the temperature range of -60 – 210 °C. The dielectric measurement was set in the frequency range of 10^2 – 10^6 Hz. The measurement was conducted using the capacitance (C_p)–dissipation factor (D or tanδ) mode. The value of ε' was calculated using the equation,

$$\varepsilon' = \frac{C_p d}{\varepsilon_0 A}, \quad (1)$$

where ***d*** and ***A*** are the sample thickness and electrode area, respectively.

ε_0 is the permittivity of free space (8.854×10^{-12} F/m). The complex impedance (Z^*) was derived from the equation involving the complex dielectric constant (ε^*),

$$\varepsilon^* = \varepsilon' - i\varepsilon'' = (i\omega C_0 Z^*)^{-1} = [i\omega C_0(Z' - iZ'')]^{-1} \quad (2)$$

where ε' and ε'' represent the real and imaginary parts of ε^*. Z' and Z'' represent the real part and imaginary part of Z^*, respectively.

$C_0 = \varepsilon_0 A/d$ is the empty cell capacitance.

RESULTS AND DISCUSSION

First of all, the phase composition and crystal structure of all the sintered CCTO and CCTO-C/T ceramics were studied using the XRD technique. As shown in Fig. 1, the primary phase of CCTO was detected in both samples even when the molar ratio of Cu and Ti was deviated from 3:4. The second phase of TiO_2 was detected in the CCTO-C/T ceramic. This result is similar to that observed in the TiO_2–rich $CaCu_3Ti_{4+x}O_{12}$ ceramics, when the molar ratio of Ti was larger than 4.0 (Lin *et al.*, 2008; Saengvong *et al.*, 2021). This observation was a result of the excess TiO_2 present in the initial raw materials. It was found that the lattice parameters of the CCTO and CCTO–C/T ceramics were 7.399 and 7.298 Å, respectively.

The microstructures of the CCTO and CCTO–C/T ceramics were studied. Fig. 2 shows the polished surfaces of the CCTO and CCTO–C/T ceramics. A dense microstructure devoid of pores was achieved in both ceramics. As anticipated, the growth of grains in CCTO ceramics can be suppressed by reducing the Cu molar ratio (< 3.0) and/or increasing the Ti molar ratio (> 4.0). The mean grain sizes of the CCTO and CCTO-C/T ceramics were calculated to be 125.9 ± 46.9 and 93.0 ± 26.2 μm, respectively. The grain growth in polycrystalline ceramics is usually caused by the movement of the grain boundaries, which can be enhanced by the presence of liquid phase during the sintering process (Rahaman, 2003; Lee *et al.*, 2014).

The rapid grain growth in the CCTO ceramic is generally attributed to the existence of CuO–related liquid phas (Mei *et al.*, 2008; Lee *et al.*, 2014). In the case of CCTO–C/T ceramic, the inhibited grain growth was caused by Cu–deficient and Ti–rich ratios, giving rise to the decreased liquid phase content and existence of TiO_2 phase, as shown in Fig. 1.

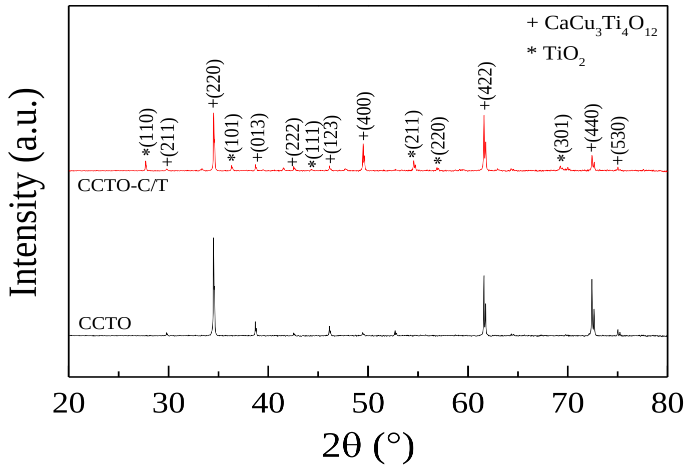

Fig. 1 XRD patterns of CCTO and CCTO-C/T ceramics.

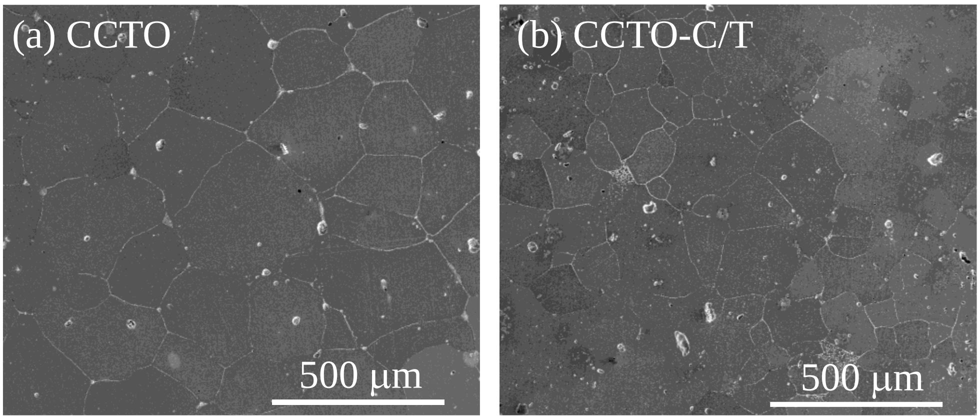

Fig. 2 SEM images of CCTO (a) and CCTO-C/T ceramics (b).

To further study the microstructure of the sintered ceramics, SEM mapping analysis was performed. As shown in Fig. 3(a), the Ca, Cu, Ti, and O elements homogeneously dispersed throughout the microstructure. However, slight segregation of CuO phase along the grain boundaries was observed in the CCTO-C/T ceramic, while Ti- and Ca-deficient were observed, as indicated by write arrows. This result may be caused by the imbalance of structure due to non-stoichiometry of the CCTO-C/T ceramic. EDS technique was used to further characterize the chemical compositions at the grain boundaries and inside the grains. As depicted in Fig. 4, the EDS spectrum detected within the grains (point-1) displayed the characteristic peaks of all elements present in the CCTO phase. However, a CuO-rich phase was observed in the EDS spectrum taken at the grain boundary (point-2). In accordance with the EDS results, the CCTO samples exhibited element percentages of 5.8 wt.% Ca, 36.5 wt.% Cu, and 28.2 wt.% Ti, respectively. For the CCTO-C/T sample, the corresponding element percentages were 6.0 wt.% Ca, 32.4 wt.% Cu, and 29.8 wt.% Ti.

The weight percentage ratios of Ti:Cu in the CCTO and CCTO-C/T samples were calculated to be 0.77 and 0.92, respectively. Evidently, the percentage ratio in the CCTO-C/T sample was larger than that in the CCTO sample, confirming Ti enrichment and Cu deficiency in the CCTO-C/T sample.

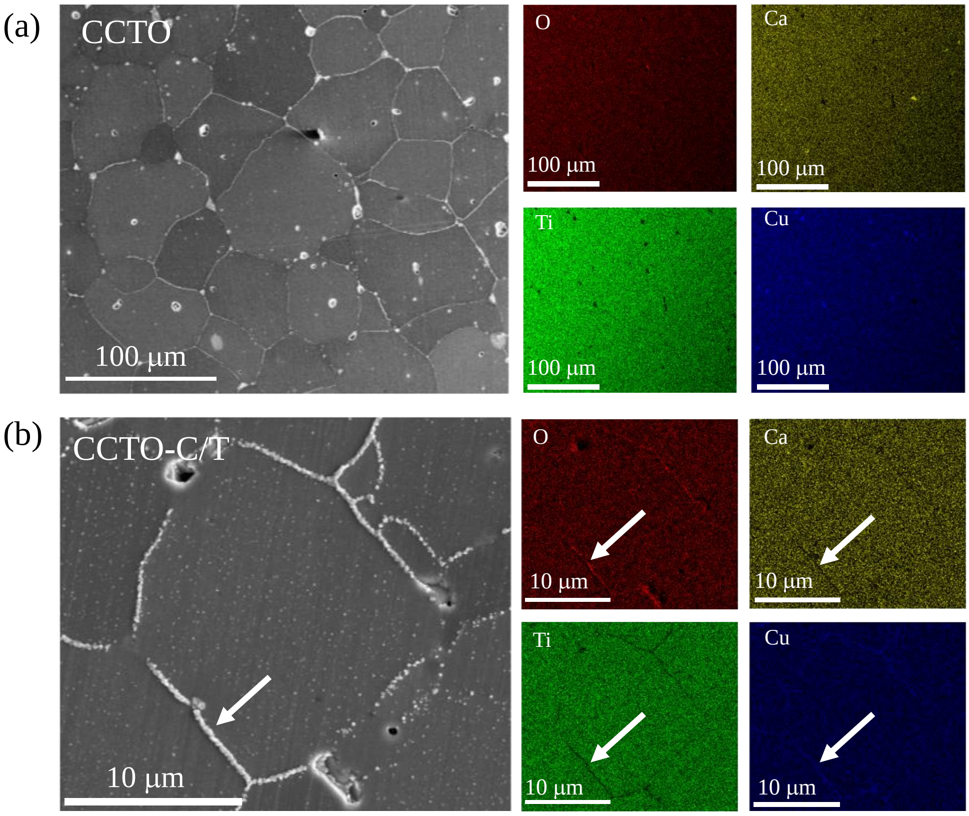

Fig. 3 SEM mapping images of all elements of CCTO (a) and CCTO-C/T ceramics (b).

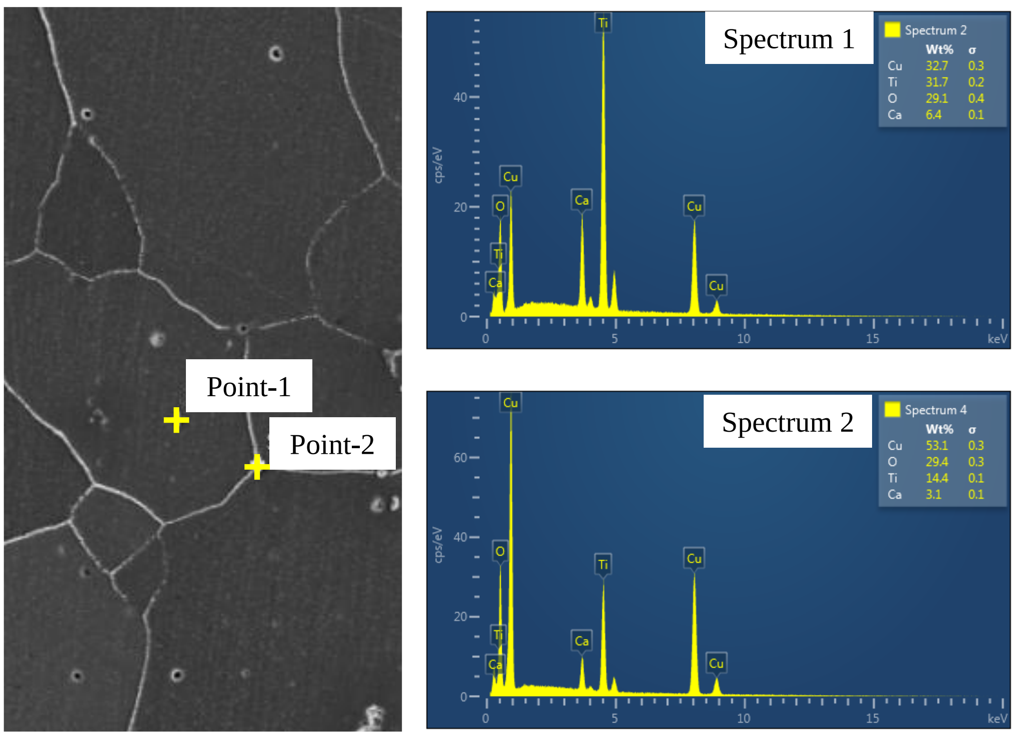

Fig. 4 SEM image of surface morphology of CCTO-C/T ceramic and EDS spectra detected at different points.

Effect Cu–deficient and Ti–rich on the giant dielectric properties was investigated. Fig. 5(a) illustrates the frequency dependence of the ε' at 25 °C. Both the ceramics exhibited the giant dielectric response. Although the ε' value of the CCTO-C/T ceramic was lower than that of the CCTO ceramic over the measured frequency, the ε' value of the CCTO-C/T ceramic was still very large (~6.58 x 10^4 at 1 kHz.). Notably, a low frequency tanδ value of the CCTO-C/T ceramic was lower that of the CCTO ceramic. At 25 °C and 1 kHz., the tanδ values of the CCTO and CCTO-C/T ceramics were 0.091 and 0.053, respectively. The giant dielectric properties can be described using the internal barrier layer capacitor (IBLC) model based on the Maxwell-Wagner polarization at the insulating grain boundaries (Liu *et al.*, 2004). The larger ε' value of the CCTO ceramic was primarily attributed to the larger mean grain size (Adams *et al.*, 2006; Wu *et al.*, 2002; Schmidt *et al.*, 2012; Vangchangyia *et al.*, 2012). Furthermore, the reduced tanδ value is usually related to the decreased grain size. It is worth noting that the rapid increase in tanδ of both ceramics in a high frequency range was due to the dielectric relaxation phenomenon (Kao, 2004; Liu *et al.*, 2004; Thongbai *et al.,* 2012), which is usually accompanied by the rapid decrease in ε' in the same frequency range.

Fig. 5(b) illustrates the dielectric properties at 1 kHz. as a function of temperature within the range of -60 to 210 °C. Remarkably, both samples exhibit a significant giant dielectric behavior across a broad spectrum of temperatures. Notably, the temperature dependence of ε' for the CCTO-C/T ceramic proves to be improved compared to that of the CCTO ceramic. At elevated temperatures, the ε' of the CCTO-C/T ceramic displays slightly less dependence on temperature when contrasted with the CCTO ceramic. Additionally, at higher temperatures, the tanδ value of the CCTO-C/T ceramic is notably lower than that of the CCTO ceramic, as shown in the inset of Fig. 5(b). The heightened ε' and tanδ values at elevated temperatures are linked to the DC conduction of free charge carriers capable of traversing the insulating grain boundary (Adams *et al.*, 2006). Consequently, the DC conduction of the CCTO-C/T ceramic is enhanced at high temperatures, rendering it well-suited for capacitor applications.

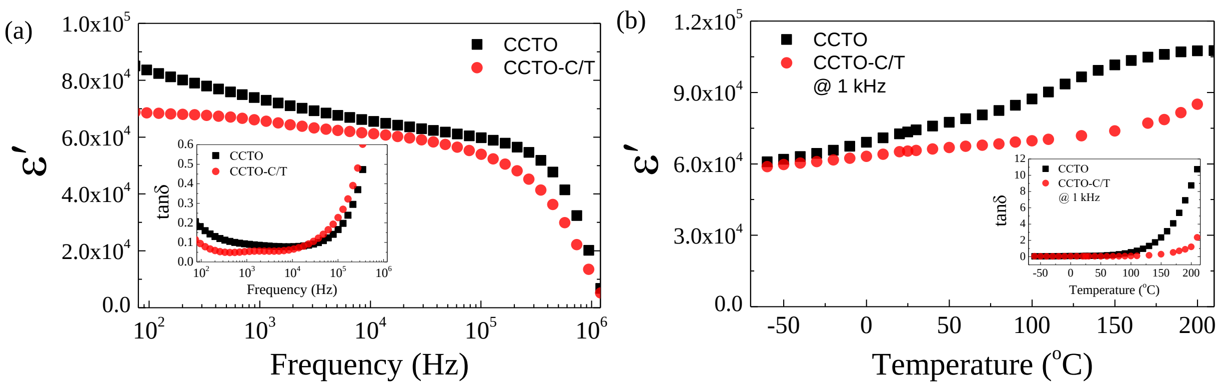

Fig. 5 ε' as a function of frequency (10^2 – 10^6 Hz.) at 25°C for the CCTO and CCTO-C/T ceramics; inset shows tanδ at 25 °C (a). ε' as a temperature (-60 – 210 °C) at 1 kHz. for the CCTO and CCTO-C/T ceramics; inset shows tanδ at 1 kHz. (b).

It has been suggested that Ti ions can substitute into the Cu site within the CCTO structure (Adams *et al.*, 2006). However, in this current study, the presence of a second phase, TiO_2, was detected in the XRD pattern of the CCTO-C/T ceramic. Consequently, we can infer that excessive Ti might not preferentially substitute into the Cu site of the CCTO structure, or Ti could substitute into the Cu site in minute quantities. Through microstructural analysis, the segregation of Cu-rich phases along the grain boundaries was observed, even when the molar ratio of CuO was lower than 3.0. Previous research (Lin *et al.*, 2008) has indicated that the presence of the TiO_2 phase can lead to a reduction in $\tan\delta$ and ε', while variations in the Cu molar ratio strongly influence changes in the resistance and capacitance of the grain boundaries, subsequently affecting the values of $\tan\delta$ and ε' (Mei *et al.*, 2008). Consequently, in cases where $x > 0.09$, it is anticipated that the ε' values would notably decrease due to excessive TiO_2 presence and Cu molar deficiency in the CCTO ceramics. Moreover, $\tan\delta$ would likely experience a significant increase because the resistance of the grain boundaries primarily correlates with the Cu ratio rather than the Ti ratio in the CCTO structure. The electrostatic potential barrier height and associated grain boundary resistance generally decrease when Cu is deficient (< 3.0). Conversely, when $x < 0.09$, observable changes in dielectric properties might not be apparent. The dielectric properties of the CCTO-C/T and CCTO ceramics were compared to those of previous works, as summarized in Table 1. As evident, the dielectric properties of CCTO-C/T are intriguing when compared to those reported previously (Cheng *et al.*, 2012; Ni and Chen, 2009; Ni and Chen, 2010).

Table 1 Comparison of the ε' and $\tan\delta$ values at approximately 25°C and 1 kHz. for CCTO and CCTO-C/T ceramics with values from previous studies.

Ceramic composition	Doping concentration (x)	ε'	$\tan\delta$	References
$CaCu_3Ti_{4-x}Ce_xO_{12}$	0.00	51,555	~0.1	(Cheng *et al.*, 2012)
	0.05	22,628	~0.3	
	0.10	916	~0.5	
	0.15	91	~7	
$CaCu_3(Ti_{1-x}Sn_x)_4O_{12}$	0.00	~35,000	~0.05	(Ni and Chen, 2009)
	0.05	~60,000	~0.04	
	0.10	~90,000	~0.04	
$Ca(Cu_{1-x}Mg_x)_3Ti_4O_{12}$	0.00	~35,000	~0.3	(Ni and Chen, 2009)
	0.05	~100,000	~0.5	
	0.10	~200,000	~0.3	
$CaCu_{3-x}Ti_{4+x}O_{12}$	0.00 (CCTO)	~32,000	0.091	In this work
	0.09 (CCTO–C/T)	~90,000	0.053	

To further elucidate the mechanism underlying the giant dielectric response in both CCTO and CCTO-C/T ceramics, Impedance Spectroscopy (IS) was conducted. Usually, IS is employed to ascertain the electrical properties of both the grains and grain boundaries (Adams *et al.*, 2006; Schmidt *et al.*, 2012). The electrical behavior of the grain boundaries can be discerned through the presence of a prominent semicircular arc within the complex impedance plane (Z*) plot. Likewise, the electrical characteristics of the grains can be deduced from the subtle semicircular arc observed at high frequencies. However, in cases where a small arc is not evident, the electrical response of the grains can still be characterized by the nonzero intercept observed on the Z'-axis. As illustrated in Fig. 6, at 25 °C, only portions of large semicircular arcs are observable within the frequency range of 40 – 10^6 Hz. for both the CCTO and CCTO-C/T ceramics. Furthermore, a nonzero intercept on the Z'-axis can be observed at high frequencies. These results are similar to those reported in literature Adams *et al.* (2006), Schmidt *et al.* (2012) and Vangchangyia *et al.* (2012), where they were identified as the electrical responses of the insulating grain boundaries and the semiconducting grains, respectively. As the temperature is raised to 60 °C, the large semicircular arcs become more prominently visible, and the nonzero intercept remains observable. Consequently, the substantial dielectric properties of both the CCTO and CCTO-C/T ceramics can be attributed to their electrically heterogeneous microstructure. When an electric field is applied across the samples, free electrons can move within the semiconducting grains but are hindered from traversing the insulating grain boundary layers. These trapped free electrons at the interface between the semiconducting grains and insulating grain boundaries lead to interfacial polarization. Consequently, significant ε' values are attainable since the dielectric response is directly tied to the strength of interfacial polarization.

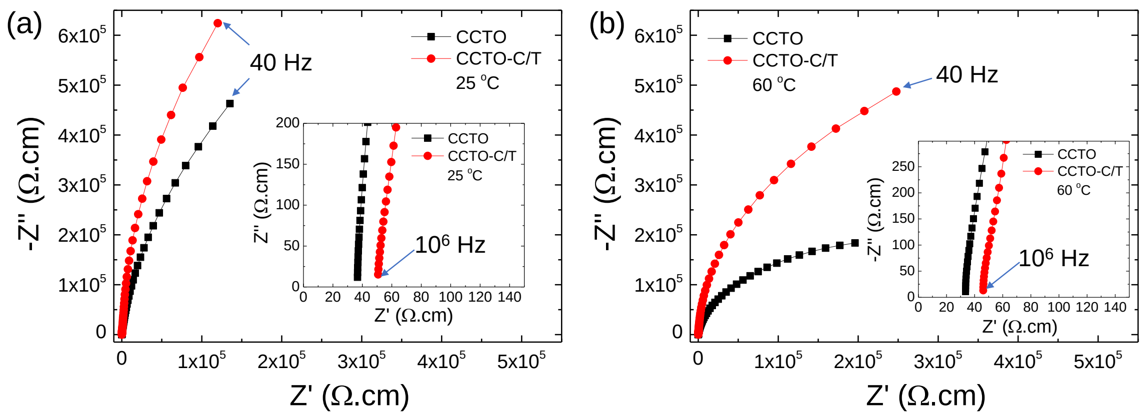

Fig. 6 Impedance complex plane (Z*) plots of CCTO and CCTO-C/T ceramics at 25 °C (a) and 60 °C; their insets Z* at high frequencies, revealing the nonzero intercept on the Z'-axis (b).

According to the IS based on the IBLC model, the grain boundary resistance and grain resistance can be calculated from the diameter of the large arc and nonzero intercept, respectively. It is important to note that the grain boundary resistance of the CCTO-C/T ceramic was larger than that of the CCTO ceramic. This result was consistent with reduced $\tan\delta$ of the CCTO-C/T ceramic. Moreover, this result is the primary cause for improving the temperature dependence on the dielectric properties of the CCTO-C/T ceramic. Usually, the low-frequency tanδ value of CCTO-based materials exhibits an inverse relationship with the resistance of the insulating grain boundary. This phenomenon accounts for the observed lower tanδ in the CCTO-C/T ceramic when compared to that of the CCTO ceramic. The presence of a segregated CuO phase along the grain boundaries and an excessive TiO_2 phase within the CCTO-C/T ceramic could potentially serve as the principal factors contributing to the heightened grain boundary resistance. Furthermore, the grain resistance of the CCTO-C/T ceramic was slightly larger than that of the CCTO ceramic. The result indicated that concentration of free electrons inside the semiconducting grains of the CCTO ceramic was higher than that of the CCTO-C/T ceramic. According to the interfacial polarization, the intensity of polarization depends on the concentration of accumulated charges at the internal interfaces (Kao, 2004; Mingmuang *et al*., 2022; Thongyong *et al*., 2023). Thus, the larger ε' value of the CCTO ceramic (compared to that of the CCTO-C/T ceramic) should be due to higher concentration of accumulated charges at the grain boundaries. It is crucial to note that the segregation of CuO and excessive TiO_2 phases could impede the occurrence of oxygen loss during the sintering process. As is widely recognized, the presence of free electrons in CCTO ceramics is commonly associated with the abundance of oxygen vacancies. Consequently, an anticipation arose that the concentration of oxygen vacancies within the CCTO-C/T ceramic would be lower compared to that within the CCTO ceramic. As a result, the grain resistance of the CCTO ceramic proved to be inferior to that of the CCTO-C/T ceramic.

CONCLUSIONS

In conclusion, the presence of the primary CCTO phase was confirmed, even when the Cu and Ti molar ratios deviated. The CCTO-C/T ceramic exhibited a secondary phase of TiO_2 and segregation of CuO along the grain boundaries. Both compositions demonstrated dense ceramics without any pores. Grain growth in CCTO ceramics was hindered by reducing the Cu molar ratio and increasing the Ti molar ratio. SEM mapping revealed a homogeneous distribution of Ca, Cu, Ti, and O elements, with slight segregation of CuO along grain boundaries and deficiencies in Ti and Ca observed in the CCTO-C/T ceramic. Both ceramics exhibited a significant giant dielectric response of ~10^4, with the CCTO-C/T ceramic displaying lower tanδ values compared to the CCTO ceramic. IS confirmed the electrical heterogeneity of the ceramics, with distinct electrical responses attributed to semiconducting grains and insulating grain boundaries. The grain boundary resistance of the CCTO-C/T ceramic was higher than that of the CCTO ceramic, whereas the grain resistance of the CCTO ceramic was lower than that of the CCTO-C/T ceramic. These differences were attributed to the segregation of CuO and excessive TiO_2 phases, which affected the grain boundary resistance and the concentration of free electrons within the semiconducting grains. The CCTO-C/T ceramic was expected to have a smaller concentration of oxygen vacancies, resulting in higher grain resistance compared to the CCTO ceramic. Overall, this study provides valuable insights into the factors influencing the microstructure and dielectric properties of CCTO and CCTO-C/T ceramics.

ACKNOWLEDGMENTS

This research has received funding support from the Research and Graduate Studies Office of Khon Kaen University and the Institute of Nanomaterials Research and Innovation for Energy (IN-RIE), Khon Kaen University.

REFERENCES

Adams, T.B., Sinclair, D.C. and West, A.R. (2006). Characterization of grain boundary impedances in fine- and coarse-grained $CaCu_3Ti_4O_{12}$ ceramics. Physical review. B, Condensed matter 73(9): 094124.

Bhardwaj, U., Sharma, A., Gupta, V., Batoo, K.M., Hussain, S. and Kushwaha, H.S. (2022). High energy storage capabilities of $CaCu_3Ti_4O_{12}$ for paper-based zinc–air battery. Scientific Reports 12(1): 3999.

Cheng, B., Lin, Y.H., Deng, W., Cai, J., Lan, J., Nan, C.W., Xiao, X. and He, J. (2012). Dielectric and nonlinear electrical behaviors in Ce-doped $CaCu_3Ti_4O_{12}$ ceramics. Journal of Electroceramics 29(4): 250 - 253.

Jumpatam, J., Prachamon, J., Boonlakhorn, J., Phromviyo, N., Chanlek, N. and Thongbai, P. (2022). Giant dielectric behavior and non-ohmic properties in $Mg^{2+}+F^{-}$ co-doped $CaCu_3Ti_4O_{12}$ ceramics. Journal of Asian Ceramic Societies. 10(2): 414 - 423.

Kao, K.C. (2004). Dielectric phenomena in solids : with emphasis on physical concepts of electronic processes. Boston: Academic Press.

Lee, S.Y., Kim, H.E. and Yoo, S.I. (2014). Subsolidus Phase Relationship in the CaO–CuO–TiO_2 Ternary System at 950°C in Air. Journal of the American Ceramic Society 97(8): 2416 - 2419.

Lin, Y.H., Cai, J., Li, M., Nan, C.W. and He, J. (2008). Grain boundary behavior in varistor-capacitor TiO_2-rich $CaCu_3Ti_4O_{12}$ ceramics. Journal of Applied Physics 103: 074111.

Liu, J., Duan, C.G., Yin, W.G., Yin, W.G., Mei W.N., Smith, R.W. and Hardy, J.R. (2004). Large dielectric constant and Maxwell-Wagner relaxation in $Bi_{2/3}Cu_3Ti_4O_{12}$. Physical review. B, Condensed matter 70(14): 144106.

Mei, L.T., Hsiang, H.I. and Fang, T.T. (2008). Effect of Copper-Rich Secondary Phase at the Grain Boundaries on the Varistor Properties of $CaCu_3Ti_4O_{12}$ Ceramics. Journal of the American Ceramic Society 91(11): 3735 - 3737.

Miao, G., Yin, M., Li, P., Hao, J., Li, W., Du, J., Li, G., Wang, C. and Fu, P. (2021). Effect of Cr addition on the structure and electrical properties of $CaCu_3Ti_4O_{12}$ NTC thermistor. Journal of Alloys and Compounds 884: 161066.

Mingmuang, Y., Chanlek, N., Moontragoon, P., Srepusharawoot, P. and Thongbai, P. (2022). Effects of Sn^{4+} and Ta^{5+} dopant concentration on dielectric and electrical properties of TiO_2: Internal barrier layer capacitor effect. Results in Physics 42: 106029.

Moulson, A.J. and Herbert, J.M. (2003). Electroceramics : materials, properties, applications, 2nd edition. New York: Wiley.

Ni, L. and Chen, X.M. (2009). Enhanced giant dielectric response in Mg-substituted $CaCu_3Ti_4O_{12}$ ceramics. Solid State Communication 149(9-10): 379 - 383.

Ni, L. and Chen, X.M. (2010). Enhancement of giant dielectric response in $CaCu_3Ti_4O_{12}$ ceramics by Zn substitution. Journal of the American Ceramic Society 93(1): 184 - 189.

Prachamon, J., Boonlakhorn, J., Chanlek, N., Phromviyo, N., Harnchana, V., Srepusharawoot, P., Swatsitang, E. and Thongbai, P. (2022). Enhanced dielectric response and non-Ohmic properties of Ge-doped $CaTiO_3/CaCu_3Ti_4O_{12}$. Journal of Asian Ceramic Societies 10(2): 473 - 481.

Rahaman, M.N. (2003). Ceramic processing and sintering, 2nd edition. New York: CRC Press.

Rai, V.S., Prajapati, D., Kumar, V., Verma, M.K., Pandey, S., Das, T., Singh, N.B. and Mandal, K.D. (2022). Low temperature synthesis, dielectric and electrical characteristics of $Bi_{2/3}Cu_{3-x}Ni_xTi_4O_{12}$ (where x = 0.05, 0.1, and 0.2) ceramics for the dielectric and electrical properties. Journal of Materials Science: Materials in Electronics 33(24): 5273 - 5282.

Saengvong, P., Chanlek, N., Putasaeng, B., Pengpad, A., Harnchana, V., Krongsuk, S., Srepusharawoot, P. and Thongbai, P. (2021). Significantly Improved Colossal Dielectric Properties and Maxwell—Wagner Relaxation of TiO_2—Rich $Na_{1/2}Y_{1/2}Cu_3Ti_{4+x}O_{12}$ Ceramics. Molecules 26(19): 6043.

Saengvong, P., Chanlek, N., Srepusharawoot, P., Harnchana, V. and Thongbai, P. (2022) Enhancing giant dielectric properties of Ta^{5+}-doped $Na_{1/2}Y_{1/2}Cu_3Ti_4O_{12}$ ceramics by engineering grain and grain boundary. Journal of the American Ceramic Society 105(27): 3447 - 3455.

Schmidt, R., Stennett, M.C., Hyatt, N.C., Pokorny, J., Prado-Gonjal, J., Li, M. and Sinclair, D.C. (2012). Effects of sintering temperature on the internal barrier layer capacitor (IBLC) structure in $CaCu_3Ti_4O_{12}$ (CCTO) ceramics. Journal of the European Ceramic Society 32(12): 3313 - 3323.

Subramanian, M.A., Li, D., Duan, N., Reisner, B.A. and Sleight, A.W. (2000). High Dielectric Constant in $ACu_3Ti_4O_{12}$ and $ACu_3Ti_3FeO_{12}$ Phases. Journal of Solid State Chemistry 151(2): 323 - 325.

Subramanian, M.A. and Sleight, A.W. (2002). $ACu_3Ti_4O_{12}$ and $ACu_3Ru_4O_{12}$ perovskites: high dielectric constants and valence degeneracy. Solid State Sciences 4(3): 347 - 351.

Thongbai, P., Jumpatam, J., Putasaeng, B., Yamwong, T. and Maensiri, S. (2012). The origin of giant dielectric relaxation and electrical responses of grains and grain boundaries of W-doped $CaCu_3Ti_4O_{12}$ ceramics. Journal of Applied Physics 112(11): 114115.

Thongyong, N., Chanlek, N., Takesada, M. and Thongbai, P. (2023). Origins of high–performance giant dielectric properties in TiO_2 co-doped with aliovalent ions via broadband dielectric spectroscopy. Results in Physics 44: 106210.

Vangchangyia, S., Swatsitang, E., Thongbai, P., Pinitsoontorn, S., Yamwong, T., Maensiri, S., Amornkitbamrung, V. and Chindaprasirt, P. (2012). Very Low Loss Tangent and High Dielectric Permittivity in Pure-$CaCu_3Ti_4O_{12}$ Ceramics Prepared by a Modified Sol-Gel Process. Journal of the American Ceramic Society 95(5): 1497 - 1500.

Wu, J., Nan, C.W., Lin, Y. and Deng, Y. (2002). Giant Dielectric Permittivity Observed in Li and Ti Doped NiO. Physical Review Letters 89(21): 217601.

Zhang, J., Zheng, J., Liu, Y., Zhang, C., Hao, W., Lei, Z. and Tian, M. (2019). The dielectric properties of CCTO ceramics prepared via different quick quenching methods. Materials Research Bulletin 115: 49 - 54.

❑❑❑❑❑